ChemComm

COMMUNICATION

View Article Online
View Journal | View Issue

Cite this: *Chem. Commun.*, 2023, **59**, 2150

Received 15th December 2022,
Accepted 23rd January 2023

DOI: 10.1039/d2cc06837k

rsc.li/chemcomm

Synthesis of a rhodium(III) dinitrogen complex using a calix[4]arene-based diphosphine ligand†

Jack Emerson-King,[a] Sudip Pan,[b] Matthew R. Gyton,[a] Ralf Tonner-Zech[b] and Adrian B. Chaplin*[a]

The synthesis and characterisation of the rhodium(III) dinitrogen complex [Rh(2,2′-biphenyl)(CxP_2)(N_2)]$^+$ are described, where CxP_2 is a *trans*-spanning calix[4]arene-based diphosphine and the dinitrogen ligand is projected into the cavity of the macrocycle.

Activation of dinitrogen by coordination to a transition metal is a process of immense biological and technological importance, helping to weaken the otherwise formidably strong nitrogen–nitrogen triple bond (D_e = 946 kJ mol^{-1}) through M→N_2 π-back donation.[1,2] Molecular dinitrogen complexes have been reported for most of the transition elements. Mononuclear d^6 systems have been the most heavily investigated, however, no well-defined rhodium(III) examples have previously been described.[3] This paucity presumably reflects an incompatibility between the weak σ-donating, poor π-accepting character of dinitrogen and the relatively high oxidation state of the second-row transition metal.

Inspired by the use of donor-functionalised cavitands as ligands in the literature and as part of our work exploring the chemistry of low-coordinate group 9 complexes supported by the high trans influence ancillary ligand 2,2′-biphenyl (biph),[4,5] we became intrigued by the prospect of using a cavitand-based ligand to isolate a labile rhodium(III) dinitrogen complex.[6] To this end, synthesis of [Rh(biph)(CxP_2)(N_2)][Al(OR^F)$_4$] (**1-N_2**, R^F = $C(CF_3)_3$; Fig. 1A) was targeted, reasoning that the previously reported diphosphine ligand CxP_2 would position the {Rh(biph)}$^+$ fragment across the upper rim of the constituent calix[4]arene scaffold and in doing so favour coordination of the small diatomic over solvent molecules. Only polynuclear and dinuclear derivatives of CxP_2 have been reported previously.[7] We herein describe the synthesis and characterisation of **1-N_2** through dehydration of the corresponding rhodium(III) aqua complex **1-OH_2**, which can be obtained in 44% isolated yield by ligand substitution of *trans*-[Rh(biph)(PPh_3)$_2$(OH_2)][Al(OR^F)$_4$] (**2-OH_2**) with CxP_2 in THF at room temperature (Fig. 1A).

In CD_2Cl_2 solution, isolated **1-OH_2** is characterised by time-averaged C_{2v} symmetry and a doublet ^{31}P resonance at δ 13.2 ($^1J_{RhP}$ = 120 Hz) at 298 K. Coordination of water within the calix[4]arene cavity is evidenced by a singlet 2H resonance at δ 0.84, which was washed out upon shaking with D_2O and is significantly shielded relative to free water (δ 1.53) and **2-OH_2** (δ 2.44). Crystals of **1-OH_2** suitable for analysis by single crystal X-ray diffraction were obtained from CH_2Cl_2-hexane and demonstrate that the metal adopts a square pyramidal coordination geometry with the CxP_2 ligand bound with near ideal trans geometry (P20–Rh1–P40 = 171.90(2)°) in the solid state (Fig. 1B). The coordinated water ligand is projected into the calix[4]arene cavity with a Rh1–O1 bond distance of 2.2046(14) Å and approximately linear C15–Rh1–O1 angle of 172.17(8)°. The formally vacant coordination site of the metal centre is sterically occluded by two phenyl groups of the CxP_2 ligand, with carbon contacts >3.4 Å suggesting that any stabilisation by agostic bonding is minimal.[8] In any case, these phenyl groups complete the encapsulation of the aqua ligand, which is contained within an almost uninterrupted van der Waals surface defined by the components of **1**.

Treatment of **1-OH_2** with an excess of the potent drying agent [$ZrCp_2Me_2$][9] in CD_2Cl_2 under an atmosphere of dinitrogen resulted in smooth conversion into a 6 : 5 dynamic equilibrium mixture of new rhodium(III) CxP_2 complexes we assign as **1-N_2** (δ_{31P} 16.1, $^1J_{RhP}$ = 117 Hz) and **1-DCM** (δ_{31P} 4.4, $^1J_{RhP}$ = 117 Hz) within 24 h at room temperature. These assignments were substantiated by freeze-pump-thaw degassing the solution to remove dinitrogen and a control reaction carried out under an atmosphere of argon, both of which resulted in exclusive formation of **1-DCM**. Highlighting the decisive role of the calix[4]arene scaffold, the spectroscopic characteristics of the bis(triphenylphosphine) analogue *trans*-[Rh(biph)(PPh_3)$_2$

[a] *Department of Chemistry, University of Warwick, Gibbet Hill Road, Coventry, CV4 7AL, UK. E-mail: a.b.chaplin@warwick.ac.uk*
[b] *Wilhelm-Ostwald-Institut für Physikalische und Theoretische Chemie, Universität Leipzig, Linnéstraße 2, Leipzig, D-04103, Germany*

† Electronic supplementary information (ESI) available: Experimental and computational details (PDF) and optimised geometries (XYZ). CCDC 2225292 (**1-OH_2**), 2225293 (**1-N_2**). For ESI and crystallographic data in CIF or other electronic format see DOI: https://doi.org/10.1039/d2cc06837k

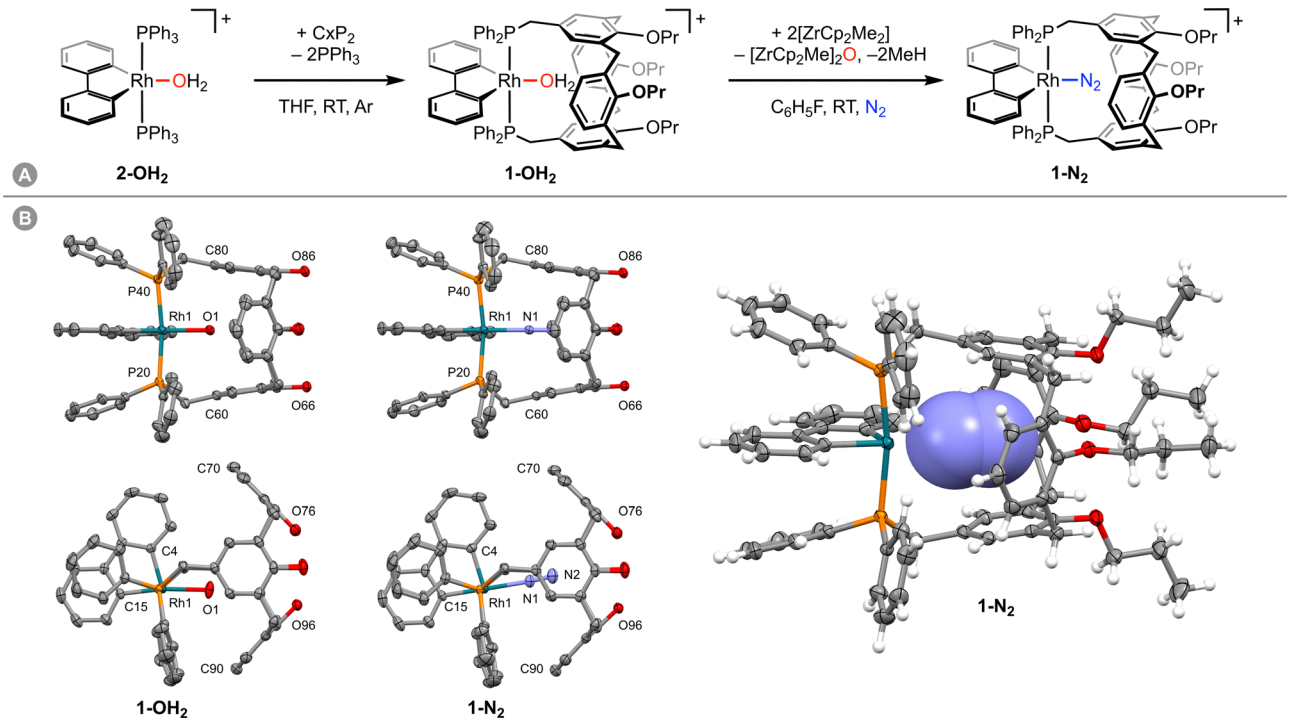

Fig. 1 (A) Synthesis of **1-N$_2$**. $[Al(OR^F)_4]^-$ counterions omitted. (B) Solid-state structures of **1-OH$_2$** and **1-N$_2$** with thermal ellipsoids at 50% probability; solvents, and anions omitted. Two perspective views shown for each complex without H atoms and Pr groups, with a third for **1-N$_2$** showing encapsulated N_2 in space fill with minor disordered components omitted (2×Pr). Selected bond lengths (Å) and angles (°): **1-OH$_2$**, Rh1–O1, 2.2046(14); Rh1–C4, 1.982(2); Rh1–C15, 1.996(2); C15–Rh1–O1, 172.17(7); Rh1–P20, 2.3505(5); Rh1–P40, 2.3403(5); P20–Rh1–P40, 171.90(2); shortest Rh1–C(phenyl), 3.485(2); **1-N$_2$**, Rh1–N2, 2.160(2); N1–N2, 1.091(3); Rh1–N1–N2, 176.7(2); Rh1–C4, 2.000(2); Rh1–C15, 2.009(2); C15–Rh1–N1, 179.43(10); Rh1–P20, 2.3732(6); Rh1–P40, 2.3630(6); P20–Rh1–P40, 169.79(2); shortest Rh1–C(phenyl), 3.470(3).

(κ^1-ClCH$_2$Cl)][Al(OR^F)$_4$] (**2-DCM**) are unchanged under an atmosphere of dinitrogen. Encouraged by these findings, the reaction between **1-OH$_2$** and [ZrCp$_2$Me$_2$] was repeated under an atmosphere of dinitrogen in the more weakly coordinating solvent fluorobenzene.[10] Consistent with our interpretation so far, **1-N$_2$** (δ_{31P} 16.0; $^1J_{RhP}$ = 116 Hz) was the only dehydration product observed by NMR spectroscopy.[11] Subsequent analysis of **1-N$_2$** by solution-phase IR spectroscopy provided direct evidence for coordination of dinitrogen. A very low intensity signal was observed at 2290 cm^{-1} and is tentatively assigned to the ν(N≡N) band. This band is red-shifted relative to free N_2 (2330 cm^{-1}), but considerably higher frequency than previously reported for terminal group 9 examples (1910–2236 cm^{-1}).[1,3] The assignment is supported by exposure of the sample to air, which resulted in disappearance of the ν(N≡N) band and formation of **1-OH$_2$** within 5 seconds, slow evaporation of the solvent and analysis of the residue by ATR-IR spectroscopy within a dinitrogen filled glovebox, and computational analysis.

Despite numerous attempts, our efforts to isolate analytically pure samples of **1-N$_2$** from solution were frustrated by the extremely strong affinity of **1** for water, resulting in contamination of samples with **1-OH$_2$** by reaction with adventurous water.[12] In one instance we were, however, able to obtain a single crystal of **1-N$_2$** suitable for analysis by X-ray diffraction, by slow diffusion of hexane into a CH_2Cl_2 solution of **1-N$_2$** generated *in situ* using [ZrCp$_2$Me$_2$] (Fig. 1B). The dinitrogen ligand was readily located from the Fourier difference map, was freely refined with 100% crystallographic occupancy, and there is no evidence for significant disorder (Fourier peaks <0.5 e Å^{-3}). Whilst this crystal was not representative of the bulk of the sample, it is the first structurally characterised example of a rhodium(III) dinitrogen complex. The solid-state structure of **1-N$_2$** is isomorphous to **1-OH$_2$** and the bulk geometric features of the {Rh(biph)(CxP$_2$)}$^+$ fragment are consequently similar. There are, however, statistically significant perturbations to the metal-centred metrics. For instance, the Rh1–P20 (2.3732(6) *vs.* 2.3505(5) Å) and Rh1–P40 (2.3630(6) *vs.* 2.3403(5) Å) bonds are elongated in **1-N$_2$**, whilst the P20–Rh1–P40 bond angle is contracted (169.79(2) *vs.* 171.90(2)°) relative to **1-OH$_2$**. Coordination of dinitrogen is also associated with a straighter C15–Rh1–N1 angle (179.43(10)°) than the corresponding metric in **1-OH$_2$** (172.17(7)°), presumably to accommodate the linear diatomic within the calix[4]arene cavity. Both terminal and bridging end-on rhodium(I) dinitrogen complexes have been structurally characterised in the solid-state by X-ray diffraction, with the corresponding Rh–N bond lengths ranging from 1.85 to 2.08 Å (CSD *version* 5.43).[13] Consistent with weak binding to the higher metal oxidation state, the Rh1–N1 bond length observed in **1-N$_2$** is substantially longer than all these examples (2.160(2) Å). As for the aqua derivative, **1-N$_2$** is fluxional in solution on the NMR time scale, adopting time-averaged C_{2v} symmetry in solution at 298 K. We attempted to

probe coordination of dinitrogen by ^{15}N NMR spectroscopy using an isotopically enriched sample in fluorobenzene, but only free dinitrogen was observed. Presumably ligand exchange is fast on the timescale of the NMR experiment at 298 K.

To help delineate the role of the calix[4]arene scaffold, a DFT-based energy decomposition analysis was performed in combination with natural orbitals for chemical valence (EDA-NOCV; PBE-D3(BJ)/TZ2P-ZORA level of theory) using minimum energy structures of **1-L** and **2-L** (L = H_2O, N_2, DCM; optimised at the PBE-D3(BJ)/def2-SVP level of theory).[14] Consistent with our hypothesis that CxP_2 destabilises solvent over dinitrogen coordination, the calculated bond dissociation energies (D_e/kJ mol^{-1}) decrease in the order H_2O (89.6) > DCM (71.3) > N_2 (68.6) for the bis(triphenylphosphine) complexes **2-L**, but H_2O (118.9) > N_2 (81.9) ≫ DCM (33.9) for **1-L**. Dichloromethane is not only too large to be accommodated within the calix[4]arene scaffold in **1**, but requires a destabilising conformational change to permit metal coordination adjacent to the upper rim of the macrocycle (ΔE_{prep} = +50.7, *cf.* +16.4 kJ mol^{-1} for **2**). The interaction between **1** and dinitrogen is characterised by a greater extent of σ-donation ($\Delta E_{L\rightarrow M}$ = 48.9%) than π-back bonding ($\Delta E_{M\rightarrow L}$ = 44.6%) and no meaningful covalent interactions with the cavity were identified from the NOCV analysis (Fig. S38, ESI†). This net charge transfer to the metal is unusual for dinitrogen complexes observed in the condensed phase, but in line with the high N≡N stretching frequency measured.[15]

In summary, structural and spectroscopic characterisation of a well-defined rhodium(III) dinitrogen complex is reported. This complex is notable for a remarkably long rhodium–nitrogen bond (2.160(2) Å), a high N≡N vibrational band (2290 cm^{-1}), and showcases the utility of donor-functionalised cavitands for interrogating small molecular activation reactions mediated by transition metals.

We thank Andy Ashley (Imperial College London) for supply of $^{15}N_2$. We gratefully acknowledge the EPSRC (DTA studentship to J. E.-K.), European Research Council (ERC, grant agreement 637313; M. R. G.), and Royal Society (UF100592, UF150675, A. B. C.) for financial support. Crystallographic data were collected using an instrument that received funding from the ERC under the European Union's Horizon 2020 research and innovation programme (grant agreement no. 637313). Computational resources were provided by ZIH Dresden and GOETHE-CSC Frankfurt.

Conflicts of interest

The authors declare no conflicts of interest.

Notes and references

1 *Transition Metal-Dinitrogen Complexes – Preparation and Reactivity*, ed. Y. Nishibayashi, Wiley-VCH, 2019.
2 (*a*) L. S. Yamout, M. Ataya, F. Hasanayn, P. L. Holland, A. J. M. Miller and A. S. Goldman, *J. Am. Chem. Soc.*, 2021, **143**, 9744–9757; (*b*) P. L. Holland, *Chem. Rev.*, 2020, **120**, 4919–4920; (*c*) J. G. Chen, R. M. Crooks, L. C. Seefeldt, K. L. Bren, R. M. Bullock, M. Y. Darensbourg, P. L. Holland, B. Hoffman, M. J. Janik, A. K. Jones, M. G. Kanatzidis, P. King, K. M. Lancaster, S. V. Lymar, P. Pfromm, W. F. Schneider and R. R. Schrock, *Science*, 2018, **360**, eaar6611; (*d*) J. W. Erisman, M. A. Sutton, J. Galloway, Z. Klimont and W. Winiwarter, *Nat. Geosci.*, 2008, **1**, 636–639.
3 Crystallographically charactered terminal rhodium dinitrogen complexes: (*a*) J. T. Moore and C. C. Lu, *J. Am. Chem. Soc.*, 2020, **142**, 11641–11646; (*b*) I. Fujii, K. Semba, Q.-Z. Li, S. Sakaki and Y. Nakao, *J. Am. Chem. Soc.*, 2020, **142**, 11647–11652; (*c*) R. Kawakami, S. Kuriyama, H. Tanaka, K. Arashiba, A. Konomi, K. Nakajima, K. Yoshizawa and Y. Nishibayashi, *Chem. Commun.*, 2019, **55**, 14886–14889; (*d*) C. Rebreyend, Y. Gloaguen, M. Lutz, J. I. van der Vlugt, I. Siewert, S. Schneider and B. de Bruin, *Chem. – Eur. J.*, 2017, **23**, 17438–17443; (*e*) N. Zhang, R. S. Sherbo, G. S. Bindra, D. Zhu and P. H. M. Budzelaar, *Organometallics*, 2017, **36**, 4123–4135; (*f*) G. M. Adams, F. M. Chadwick, S. D. Pike and A. S. Weller, *Dalton Trans.*, 2015, **44**, 6340–6342; (*g*) M. G. Scheibel, Y. Wu, A. C. Stückl, L. Krause, E. Carl, D. Stalke, B. de Bruin and S. Schneider, *J. Am. Chem. Soc.*, 2013, **135**, 17719–17722; (*h*) O. V. Zenkina, E. C. Keske, R. Wang and C. M. Crudden, *Angew. Chem., Int. Ed.*, 2011, **50**, 8100–8104; (*i*) J. Schöffel, N. Šušnjar, S. Nückel, D. Sieh and P. Burger, *Eur. J. Inorg. Chem.*, 2010, 4911–4915; (*j*) S. K. Hanson, D. M. Heinekey and K. I. Goldberg, *Organometallics*, 2008, **27**, 1454–1463; (*k*) J. M. Praetorius, R. Wang and C. M. Crudden, *Eur. J. Inorg. Chem.*, 2009, 1746–1751; (*l*) A. Y. Verat, M. Pink, H. Fan, J. Tomaszewski and K. G. Caulton, *Organometallics*, 2008, **27**, 166–168; (*m*) J. D. Masuda and D. W. Stephan, *Can. J. Chem.*, 2005, **83**, 324–327; (*n*) A. Vigalok, H. Kraatz, L. Konstantinovsky and D. Milstein, *Chem. – Eur. J.*, 1997, **3**, 253–260; (*o*) P. R. Hoffman, T. Yoshida, T. Okano, S. Otsuka and J. A. Ibers, *Inorg. Chem.*, 1976, **15**, 2462–2466.
4 (*a*) G. R. F. Orton, B. S. Pilgrim and N. R. Champness, *Chem. Soc. Rev.*, 2021, **50**, 4411–4431; (*b*) D. Matt and J. Harrowfield, *ChemCatChem*, 2021, **13**, 153–168; (*c*) S. H. A. M. Leenders, R. Gramage-Doria, B. de Bruin and J. N. H. Reek, *Chem. Soc. Rev.*, 2015, **44**, 433–448; (*d*) C. Gibson and J. Rebek, *Org. Lett.*, 2002, **4**, 1887–1890; (*e*) C. Wieser-Jeunesse, D. Matt and A. D. Cian, *Angew. Chem., Int. Ed.*, 1998, **37**, 2861–2864.
5 (*a*) T. M. Hood and A. B. Chaplin, *Dalton Trans.*, 2021, **50**, 2472–2482; (*b*) M. R. Gyton, A. E. Kynman, B. Leforestier, A. Gallo, J. R. Lewandowski and A. B. Chaplin, *Dalton Trans.*, 2020, **49**, 5791–5793; (*c*) T. M. Hood, M. R. Gyton and A. B. Chaplin, *Dalton Trans.*, 2020, **49**, 2077–2086; (*d*) T. M. Hood, B. Leforestier, M. R. Gyton and A. B. Chaplin, *Inorg. Chem.*, 2019, **58**, 7593–7601; (*e*) J. Emerson-King, I. Prokes and A. B. Chaplin, *Chem. – Eur. J.*, 2019, **25**, 6317–6319; (*f*) M. R. Gyton, B. Leforestier and A. B. Chaplin, *Organometallics*, 2018, **37**, 3963–3971; (*g*) R. C. Knighton, J. Emerson-King, J. P. Rourke, C. A. Ohlin and A. B. Chaplin, *Chem. – Eur. J.*, 2018, **24**, 4927–4938.
6 J. Emerson-King, PhD thesis, University of Warwick, 2019.
7 X. Fang, B. L. Scott, J. G. Watkin, C. A. G. Carter and G. J. Kubas, *Inorg. Chim. Acta*, 2001, **317**, 276–281.
8 M. Brookhart, M. L. H. Green and G. Parkin, *Proc. Natl. Acad. Sci. U. S. A.*, 2007, **104**, 6908–6914.
9 (*a*) N. A. Yakelis and R. G. Bergman, *Organometallics*, 2005, **24**, 3579–3581; (*b*) G. Proulx and R. G. Bergman, *Organometallics*, 1996, **15**, 684–692.
10 S. D. Pike, M. R. Crimmin and A. B. Chaplin, *Chem. Commun.*, 2017, **53**, 3615–3633.
11 Complete decomposition to an intractable precipitate *via* a transient intermediate assumed to be 'naked' **1** (δ_{31P} 17.1, $^1J_{RhP}$ = 122 Hz) was observed on a similar timescale when the reaction was repeated under an atmosphere of argon.
12 **1-N2** extracts water from vacuum dried 3 Å molecular sieves in solution.
13 The longest Rh–N bond length reported in the literature is 2.076(2) Å for a neutral rhodium(I) dimer of the form [(PBP)Rh–N≡N–Rh(PBP)]M. Hasegawa, Y. Segawa, M. Yamashita and K. Nozaki, *Angew. Chem., Int. Ed.*, 2012, **51**, 6956–6960.
14 (*a*) F. M. Bickelhaupt and E. J. Baerends, in *Reviews in Computational Chemistry*, ed. K. B. Lipkowitz and D. B. Boyd, Wiley-VCH, 2000, ch. 1, vol. 15, pp. 1–86; (*b*) L. Zhao, M. Hermann, W. H. E. Schwarz and G. Frenking, *Nat. Rev. Chem.*, 2019, **3**, 48–63; (*c*) M. P. Mitoraj, A. Michalak and T. Ziegler, *J. Chem. Theor. Comput.*, 2009, **5**, 962–975.
15 M. Schmitt and I. Krossing, *J. Comput. Chem.*, 2023, **44**, 149–158.

